



Onset of a Propagating Self-Sustained Spin Reversal Front in a Magnetic System

P. Subedi,¹ S. Vélez,² F. Macià,¹ S. Li,³ M. P. Sarachik,³ J. Tejada,² S. Mukherjee,⁴ G. Christou,⁴ and A. D. Kent¹

¹*Department of Physics, New York University, New York, New York 10003, USA*

²*Grup de Magnetisme, Departament de Física Fonamental, Universitat de Barcelona, Barcelona 08028, Spain*

³*Department of Physics, City College of New York, CUNY, New York, New York 10031, USA*

⁴*Department of Chemistry, University of Florida, Gainesville, Florida 32611, USA*

(Received 8 January 2013; published 13 May 2013)

The energy released in a magnetic material by reversing spins as they relax toward equilibrium can lead to a dynamical instability that ignites self-sustained rapid relaxation along a deflagration front that propagates at a constant subsonic speed. Using a trigger heat pulse and transverse and longitudinal magnetic fields, we investigate and control the crossover between thermally driven magnetic relaxation and magnetic deflagration in single crystals of Mn₁₂-acetate.

DOI: [10.1103/PhysRevLett.110.207203](https://doi.org/10.1103/PhysRevLett.110.207203)

PACS numbers: 75.50.Xx, 75.40.Gb, 75.60.Jk, 82.33.Vx

Raising the temperature of a flammable substance can ignite combustion, an exothermic reaction between a substance and an oxidizer that results in a chemically modified substance [1]. Deflagration is a self-sustained combustion that propagates at subsonic speed via thermal conduction; a locally burning substance increases the temperature of an adjacent unburned substance and ignites it. Deflagration is governed by local reactions and diffusion; reaction-diffusion systems are ubiquitous in nature—from cell growth to epidemics. The study of these nonlinear dynamical systems reveals rich phenomenology—including traveling waves, dissipative solitons [2], and self-organized patterns [3,4].

Magnetic relaxation is a reaction-diffusion process that can develop an instability and proceed as a magnetic deflagration. It can occur in a magnetic material prepared in a metastable spin configuration; here the reaction is the reversal of spins that releases Zeeman energy and the diffusion serves to transmit the energy to adjacent material. The phenomenon has been observed as fast magnetization jumps in molecular magnets [5,6], manganites [7], and intermetallic compounds [8]. In these systems, spins that are in a metastable state at low temperature slowly relax to a lower energy state releasing heat. In some circumstances, the heat cannot be compensated by thermal diffusion, resulting in an instability that gives rise to a front of rapidly reversing spins traveling through the sample at constant speed.

In this Letter we study the instability that leads to the ignition of magnetic deflagration in a thermally driven Mn₁₂-acetate (hereafter Mn₁₂-Ac) crystal. We explore how to control the crossover between slow magnetic relaxation and rapid, self-sustained magnetic deflagration using magnetic fields. Based on earlier work [9,10], we propose a simple model and perform numerical simulations that provide a good description of the experimental findings.

Mn₁₂-Ac molecules are magnetically bistable [11] due to their high $S = 10$ spin and a magnetic anisotropy that provides a large energy barrier between spin-up and

spin-down states [see Fig. 1(a)]. In the presence of an applied field $\mathbf{H} = (H_{\perp}, H_z)$ the simplest spin Hamiltonian has the form

$$\mathcal{H} = -DS_z^2 - g\mu_B H_z S_z - g\mu_B H_{\perp} S_{\perp}. \quad (1)$$

The first term defines the anisotropy barrier ($DS^2 \approx 65$ K) and the second and third terms specify the effect of the magnetic field applied parallel and perpendicular to the anisotropy axis. As shown in Fig. 1(a), the energy barrier between the metastable and the stable state is the activation energy U , and the energy released by the reversing spins is the Zeeman energy $\Delta E = 2g\mu_B H_z S_z$. The transverse field H_{\perp} reduces the activation energy and mixes eigenstates of S_z leading to relaxation by quantum tunneling of magnetization, particularly at specific resonant values of the magnetic field [$H_z = kD/(g\mu_B) \approx 0.45k$ T, for integer k], corresponding to the crossings of energy levels with opposite spin projections. The longitudinal field H_z biases the potential well also reducing the activation energy and increasing the relaxation rate.

The abrupt complete reversal of the magnetic moment of Mn₁₂-Ac crystals was first reported by Paulsen and Park [12] and later shown to take the form of a propagating spin-reversal front [5]. Magnetic deflagration has been studied

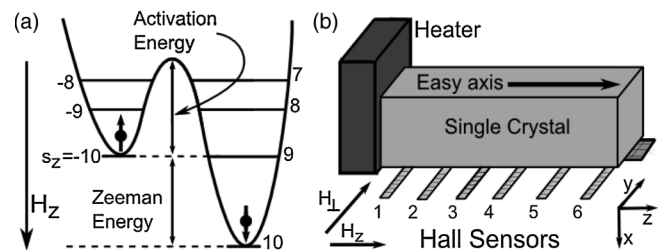


FIG. 1. (a) Potential energy showing discrete energy levels of Mn₁₂-Ac spin Hamiltonian [Eq. (1)]. (b) Schematic of the sample, Hall sensors, heater, and the directions of the applied magnetic fields.

by sweeping the magnetic field or by raising the crystal's temperature. Thresholds for both temperature [13] and applied Zeeman fields [14] were found to be governed by quantum laws due to quantum tunneling of magnetization [15]. In the experiments reported below, the spin reversal was triggered using a heat pulse at one end of the sample.

Magnetic measurements were performed on three $\text{Mn}_{12}\text{-Ac}$ single crystals of dimensions $\sim 0.3 \times 0.3 \times 2.1 \text{ mm}^3$, $0.35 \times 0.35 \times 1.75 \text{ mm}^3$, and $0.4 \times 0.4 \times 1.6 \text{ mm}^3$ (samples A, B, and C, respectively). The samples were mounted on a one-dimensional array of Hall sensors (active area $20 \times 100 \text{ }\mu\text{m}^2$ with $200 \text{ }\mu\text{m}$ separation) [see Fig. 1(b)]. The three samples show essentially the same behavior; here we show data for sample C. Care was taken to align the sample and the Hall array (placed in the yz plane) relative to each other and relative to the magnet axes, as shown in Fig. 1(b). The Hall sensors detect the stray field B_x [see the inset of Fig. 2(b)], which is maximum at the reversal front. Measurements were taken at 0.4 K in a ^3He refrigerator in a three-dimensional vector superconducting magnet capable of producing bipolar bias fields up to 1 T and bipolar transverse fields up to 5 T. A 6 V, 30 ms pulse was applied to a thin film heater ($R \approx 1.32 \text{ k}\Omega$ at 0.4 K) placed at one end of the sample to trigger spin reversal. A dc current of $20 \text{ }\mu\text{A}$ was supplied to the array of Hall sensors and the signal from each sensor was amplified by a factor of 1000, filtered, and recorded by a data acquisition card.

At base temperature (0.4 K), the crystal was prepared in a fully magnetized state so that all the spins were aligned in one direction. A fixed H_{\perp} was applied and H_z was swept

to the desired field and held. At this low temperature the spins are essentially blocked by the strong magnetic anisotropy of $\text{Mn}_{12}\text{-Ac}$, and relax slowly toward equilibrium. In this nonequilibrium state, we supplied a voltage pulse to the heater to increase the temperature at one end of the crystal to initiate spin reversal. The same pulse was used to trigger the data acquisition card to record the magnetization signals of different Hall sensors during 1 s. The procedure was repeated for several values of H_z for a particular H_{\perp} .

Figure 2 shows the time evolution of the Hall sensor signals when a heat pulse is applied at $t = 0$ to sample C with the magnetization prepared as described above. Two cases are considered: a zero bias field [$H_z = 0 \text{ T}$; see Fig. 2(a)], and a large bias field [$H_z = 0.61 \text{ T}$; see Fig. 2(b)] for the same transverse field $H_{\perp} = 1.5 \text{ T}$. A propagating spin-reversal region is observed in both cases; the change in magnetization always starts at the heater end and propagates towards the other end [from the 1st to the 6th sensor; see Fig. 1(b)]. As shown in Fig. 2, a peak in the signal corresponding to the enhancement of the local stray field (B_x) travels in the z direction as the spin reversal propagates along the easy axis, ultimately reversing the magnetization of the entire crystal. The speed of propagation of the reversing spins can be determined from the time difference between pulses sensed by adjacent Hall sensors and their separation.

While the curves in Figs. 2(a) and 2(b) appear similar, closer inspection shows that the reversal processes at low and high bias are distinctly different. At zero (or low) bias, the time interval between adjacent peaks is relatively long and increases as the spin reversal propagates, indicating that the spin reversal is slowing down: the time to completion is on the order of 80 ms, and the peaks are fairly broad and broaden further as the reversal proceeds. Here the spin reversal propagates slowly and its speed decreases because the magnetization relaxes toward equilibrium following the heat pulse; its progress through the crystal is governed by thermal diffusivity.

By contrast, in the case of high bias shown in Fig. 2(b), the time between adjacent peaks is constant and on the order of $100 \text{ }\mu\text{s}$, corresponding to a constant speed of $v \sim 2 \text{ m/s}$, consistent with the data measured by Suzuki *et al.* [5], the total time for reversal of the full magnetization of the crystal is of the order of 1 ms, and the peaks in Fig. 2(b) are substantially sharper and do not broaden as they travel. The constant speed in the case of a large H_z is a signature of magnetic deflagration, a self-sustained process driven by the Zeeman energy released by the spins as they reverse.

We will now show that the crossover between these two regimes is surprisingly sharp. The speed of propagation of the spin-reversal fronts was determined from the time interval between maxima of the Hall sensors in the middle of the crystal (sensor 3 and 4) and their spatial separation.

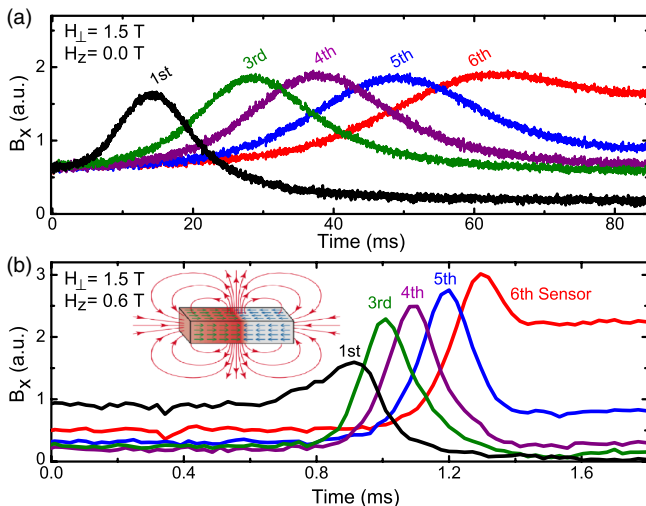


FIG. 2 (color online). Signals of the Hall sensor arrays as a function of time. (a) At zero bias field, the peaks are very broad, the propagation time is long and the speed is not constant. (b) At $H_z = 0.61 \text{ T}$, the peaks are sharp and spin reversal propagates at higher and constant speed. The inset shows stray fields from the sample when the reversal front is in the middle of the crystal. The maximum B_x is at the position of the front.

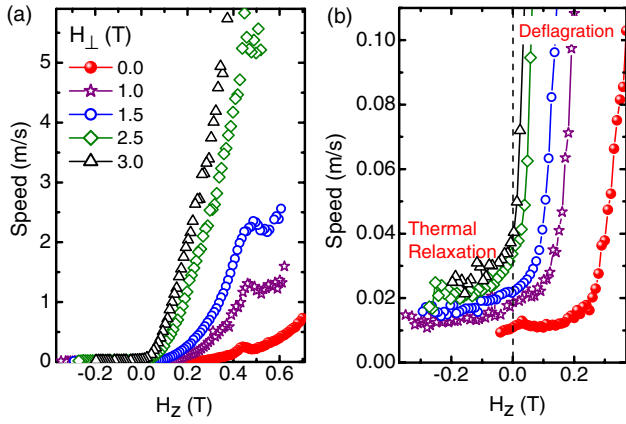


FIG. 3 (color online). (a) The speed of propagation of the spin reversal as a function of H_z for different H_\perp . (b) A blow up of the data for small H_z . The speed is small and nearly constant at very small H_z and increases abruptly when a deflagration develops.

Note that while the same speed is obtained using any pair of Hall sensors for large H_z , the speed varies from point to point at low H_z , and therefore between different Hall sensor pairs. As shown in Fig. 3, the speed of the spin-reversal front changes abruptly at a bias field that depends on the transverse field. For a given H_\perp , below a crossover bias field H_{co} (for, e.g., $H_{co} = 0.25$ T for $H_\perp = 0$ T), the speed of propagation of the reversing spins is nearly independent of the bias field. However, above the crossover, the speed increases suddenly and depends strongly on the bias field. Figure 3(b), a magnification of Fig. 3(a) where the vertical scale has been expanded by a factor of 100, demonstrates this even more clearly.

The peaks in the speed at $H_z \sim 0.45$ T shown in Fig. 3(a) are a clear manifestation of the important influence of quantum mechanics on the dynamics of the system. These maxima are due to quantum tunneling at the resonant fields [15,16] whenever spin states on opposite sides of the anisotropy barrier have nearly the same energy. As noted earlier, tunneling enhances relaxation and effectively reduces the anisotropy barrier. As we increase H_\perp we increase the tunnel splitting between levels, which results in a broadening of the resonance steps. A small peak can also be seen in Fig. 3(b) at the zero bias resonance. Note that the zero-field resonance is slightly shifted (~ 40 mT) due to internal dipolar fields [17,18].

To better understand the crossover between the two regimes described above, we develop a simple model based on previous theory [9,10,19]. The reaction-diffusion system that describes the time evolution of the magnetization m towards equilibrium m_{eq} entails two processes: the Zeeman energy (i.e., heat) released into the sample by the spins as they reverse and the heat diffusion through the sample. The dynamical system of nonlinear partial differential equations reads

$$\dot{m} = -\Gamma(m - m_{eq}), \quad \dot{T} = \dot{m}\Delta E/C + \nabla \cdot \kappa \nabla T. \quad (2)$$

Here T is the temperature, κ is the thermal diffusivity, C is the heat capacity, and $\Gamma = \Gamma_0 \exp[-U(h_\perp, h_z)/(k_B T)]$ is the relaxation rate. For fields that are much smaller than the anisotropy field ($h_i = g\mu_B H_i/2DS \ll 1$) [20]

$$U(h_\perp, h_z) \approx DS^2(1 - h_z)^2 \left[1 - 2h_\perp \frac{(1 - h_z^2)^{1/2}}{(1 - h_z)^2} \right]. \quad (3)$$

For some applied fields and initial conditions, the thermal diffusivity cannot compensate for the increase in temperature due to the Zeeman energy released by the reversing spins; the sample temperature then rapidly increases and a magnetic deflagration develops. To study the ignition of magnetic deflagration, we consider a system of spins blocked in a given metastable magnetic state, increase its temperature T_s (e.g., from $T_s = 0.5$ to 6 K), and study the resulting nucleation process. Let us consider here for simplicity the temperature evolution in a nucleation volume, independent of coordinates,

$$\dot{T} = \dot{m}\Delta E/C - 2\kappa(T - T_s)/R^2, \quad (4)$$

where T is the temperature of the volume under study and $2R$ is the characteristic size of the nucleation volume. The negative term in Eq. (4) is linear with temperature while the reaction term increases exponentially with temperature $\{\dot{m} \propto \exp[-U/(k_B T)]\}$; there is thus a competition between these two terms and stationary solutions ($\dot{T} = 0$) correspond to temperatures when the dissipation equals the released energy.

As shown in the inset of Fig. 4, some magnetic field configurations [$\mathbf{H} = (H_\perp, H_z)$] corresponding to small bias fields have stationary solutions (red dotted curve). As we vary \mathbf{H} (i.e., we vary the relaxation rate \dot{m}), the

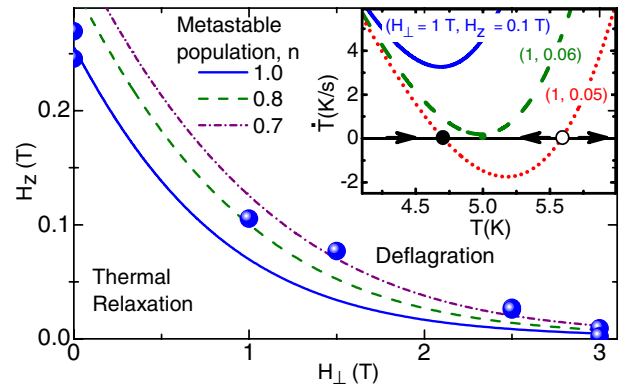


FIG. 4 (color online). The main panel shows boundary curves separating thermal and Zeeman regimes. The different curves denote different initial metastable spin populations $n = (M_s - m)/(2M_s)$, where M_s is saturation magnetization. The blue dots are crossover fields derived from the data in Fig. 3. The inset shows \dot{T} as a function of T for three different \mathbf{H} . The solid and open black circles indicate stable and unstable solutions for the case $\mathbf{H} = (1, 0.05)$ T.

stationary points move closer to each other and eventually merge (green dashed curve) and disappear. When there is no stationary solution (blue solid line)—the temperature derivative is always positive leading to an instability—a magnetic deflagration may develop. The condition for the crystal to lose stability at a given T_s and \mathbf{H} is $\dot{T} > 0$ and its crossover points are found by solving

$$\dot{T} = 0, \quad \partial \dot{T} / \partial T = 0. \quad (5)$$

At a given H_\perp , for $H_z < H_{co}$, the energy released during the spin-reversing process is small (or even zero in the case of zero bias). The dynamics of the propagating front observed in this case [see Fig. 2(a)] are determined by the diffusion of the heat supplied by the heater pulse; this corresponds to a thermal regime. Here the reaction term in Eq. (4) is negligible and the equation has a stable solution at a temperature close to the sample temperature. Neglecting the reaction term in the full set of Eqs. (2), it is clear that the heat diffuses and the magnetization locally follows the sample temperature.

For $H_z \geq H_{co}$, the energy released by the reversing spins is large, the reaction term dominates over the diffusion term, and Eq. (4) displays an instability. In this Zeeman regime, the released energy drives the spin relaxation to a deflagration with steady propagation, where the speed of the propagating front of reversing spins strongly depends on both H_z and H_\perp .

The sharp transition in propagation speed from thermal to Zeeman regimes as a function of the applied magnetic field is given by the condition in Eqs. (5). H_\perp varies the activation barrier and does not change the released energy; it affects only \dot{m} in the reaction term. H_z affects both \dot{m} and ΔE .

In the main panel of Fig. 4, we plot the boundaries that separate the thermal regime from the Zeeman regime derived from Eq. (5) together with the experimental points (blue dots) obtained from Fig. 3. For fields above the boundary curve, the reaction term dominates and the crystal develops a magnetic deflagration; below the curves, thermal diffusion dominates and the spins evolve toward equilibrium through slow thermal relaxation. For the calculations we have taken as free parameters the temperature T_s to which we heat one end of the sample, and the combination of thermal diffusivity and nucleation size κ/R^2 . Using a heat capacity close to the measured value $C/k_B = 1$ [i.e., $C = 8.3 \text{ J}/(\text{mol K})$] [21], and bounding $2R$ by the smallest sample dimension of $400 \mu\text{m}$, a good qualitative fit was obtained for $T_s = 6 \text{ K}$ and $\kappa = 1 \times 10^{-4} \text{ m}^2/\text{s}$, which agrees well with previously used values [22]. It is important to note that equally good fits can be obtained using different combinations of parameters.

The smoothness and reproducibility of the data in Fig. 3 suggest that the appearance of instabilities leading to a magnetic deflagration when raising the temperature of

the $\text{Mn}_{12}\text{-Ac}$ crystal is a well controlled process. Once the crystal is in the Zeeman regime the speed of the magnetic deflagration can be controlled by the strength of the applied field. Additionally, equal propagation speeds are obtained for different combinations of applied fields, as seen in Fig. 3 where a particular speed can be seen to correspond to different magnetic field configurations. Larger bias fields would produce larger amounts of heat released and higher temperatures for the overall process, while large transverse fields that speed up the process by the same amount would heat the sample much less. This illustrates the strongly anisotropic nature of deflagration in $\text{Mn}_{12}\text{-Ac}$. The anisotropic properties of magnetic deflagration have been investigated both experimentally [14,23] and theoretically [24].

To summarize, we have measured the dynamics of spin-reversal fronts in $\text{Mn}_{12}\text{-Ac}$ crystals in the presence of both bias and transverse magnetic fields. We have shown how these applied fields can be used to control an instability that separates slow magnetic relaxation from rapid, self-sustained magnetic deflagration.

We have also expanded the range of conditions under which magnetic deflagration has been observed, particularly to the case of small bias fields, which corresponds to small energy release in the deflagration process. This is a particularly interesting limit in which instabilities in the front are predicted to occur, such as pattern formation and oscillations of the propagating front [25]. In the presence of large transverse fields, where quantum tunneling dominates over thermal effects, the instabilities in the magnetization dynamics could lead to a deflagration-to-detonation transition [27,28] and may result in supersonic fronts [26]. The present experiments thus provide opportunities to study—in a nondestructive manner—a large variety of instabilities in magnetic systems.

We acknowledge illuminating discussions with Dov Levine, D. A. Garanin, and E. M. Chudnovsky. A. D. K. and P. S. acknowledge support by NSF-DMR-1006575 and NYU. F. M. acknowledges support from the EU, MC-IOF 253214. M. P. S. acknowledges support from NSF-DMR-0451605. Support for G. C. was provided under Grant No. CHE-0910472. S. V. acknowledges financial support from the Ministerio de Educación, Cultura y Deporte de España, and J. T. acknowledges financial support from ICREA Academia.

-
- [1] I. Glassman and R. Yetter, *Combustion* (Academic, New York, 2008), 4th ed.
 - [2] N. Akhmediev and A. Ankiewicz, *Dissipative Solitons* (Springer, New York, 2005).
 - [3] M. Cross and P. C. Hohenberg, *Rev. Mod. Phys.* **65**, 851 (1993).
 - [4] O. Zik, Z. Olami, and E. Moses, *Phys. Rev. Lett.* **81**, 3868 (1998).
 - [5] Y. Suzuki *et al.*, *Phys. Rev. Lett.* **95**, 147201 (2005).

- [6] A. Hernández-Mínguez, J.M. Hernandez, F. Macià, A. García-Santiago, J. Tejada, and P.V. Santos, *Phys. Rev. Lett.* **95**, 217205 (2005).
- [7] F. Macià, A. Hernández-Mínguez, G. Abril, J.M. Hernandez, A. García-Santiago, J. Tejada, F. Parisi, and P.V. Santos, *Phys. Rev. B* **76**, 174424 (2007).
- [8] S. Vélez, J.M. Hernandez, A. Fernandez, F. Macià, C. Magen, P.A. Algarabel, J. Tejada, and E.M. Chudnovsky, *Phys. Rev. B* **81**, 064437 (2010).
- [9] A. Hernandez-Mínguez, F. Macià, J.M. Hernandez, J. Tejada, L.H. He, and F.F. Wang, *Europhys. Lett.* **75**, 811 (2006).
- [10] D.A. Garanin and E.M. Chudnovsky, *Phys. Rev. B* **76**, 054410 (2007).
- [11] R. Sessoli, D. Gatteschi, A. Caneschi, and M. Novak, *Nature (London)* **365**, 141 (1993).
- [12] C. Paulsen and J. Park, *Quantum Tunneling of Magnetization* (Kluwer, Dordrecht, The Netherlands, 1995).
- [13] S. McHugh, R. Jaafar, M.P. Sarachik, Y. Myasoedov, A. Finkler, H. Shtrikman, E. Zeldov, R. Bagai, and G. Christou, *Phys. Rev. B* **76**, 172410 (2007).
- [14] F. Macià, J.M. Hernandez, J. Tejada, S. Datta, S. Hill, C. Lampropoulos, and G. Christou, *Phys. Rev. B* **79**, 092403 (2009).
- [15] J.R. Friedman, M.P. Sarachik, J. Tejada, and R. Ziolo, *Phys. Rev. Lett.* **76**, 3830 (1996).
- [16] J.M. Hernandez, X.X. Zhang, F. Luis, J. Bartolomé, J. Tejada, and R. Ziolo, *Europhys. Lett.* **35**, 301 (1996); L. Thomas, F. Lioni, R. Ballou, D. Gatteschi, R. Sessoli, and B. Barbara, *Nature (London)* **383**, 145 (1996).
- [17] S. McHugh, R. Jaafar, M.P. Sarachik, Y. Myasoedov, H. Shtrikman, E. Zeldov, R. Bagai, and G. Christou, *Phys. Rev. B* **79**, 052404 (2009).
- [18] B. Wen, P. Subedi, L. Bo, Y. Yeshurun, M.P. Sarachik, A.D. Kent, A.J. Millis, C. Lampropoulos, and G. Christou, *Phys. Rev. B* **82**, 014406 (2010).
- [19] J.M. Deutsch and A. Berger, *Phys. Rev. Lett.* **99**, 027207 (2007).
- [20] D.A. Garanin and E.M. Chudnovsky, *Phys. Rev. B* **56**, 11102 (1997).
- [21] A.M. Gomes, M.A. Novak, R. Sessoli, A. Caneschi, and D. Gatteschi, *Phys. Rev. B* **57**, 5021 (1998).
- [22] J.M. Hernandez, P.V. Santos, F. Macià, A. García-Santiago, and J. Tejada, *Appl. Phys. Lett.* **88**, 012503 (2006).
- [23] S. Vélez, J.M. Hernandez, A. García-Santiago, J. Tejada, V.K. Pecharsky, K.A. Gschneidner, D.L. Schlagel, T.A. Lograsso, and P.V. Santos, *Phys. Rev. B* **85**, 054432 (2012).
- [24] C.M. Dion, O. Jukimenko, M. Modestov, M. Marklund, and V. Bychkov, *Phys. Rev. B* **87**, 014409 (2013).
- [25] M. Modestov, V. Bychkov, and M. Marklund, *Phys. Rev. B* **83**, 214417 (2011).
- [26] D.A. Garanin and S. Shoyeb, *Phys. Rev. B* **85**, 094403 (2012).
- [27] M. Modestov, V. Bychkov, and M. Marklund, *Phys. Rev. Lett.* **107**, 207208 (2011).
- [28] W. Decelle, J. Vanacken, V.V. Moshchalkov, J. Tejada, J.M. Hernández, and F. Macià, *Phys. Rev. Lett.* **102**, 027203 (2009).